

THIRD OVERTONE QUARTZ RESONATOR

R. D. MINDLIN

89 Deer Hill Drive, Ridgefield, CT 06877, U.S.A.

(Received 30 October 1981)

Abstract—The Lee–Nikodem equations of motion of elastic plates are solved for the case of vibrations of an AT-cut quartz strip, with free faces and edges, at frequencies up to and including the third harmonic thickness-shear overtone.

1. INTRODUCTION

About 30 years ago, A. W. Warner[1] developed a high precision crystal-plate resonator utilizing the third harmonic overtone of thickness-shear vibration, i.e. a mode involving a thickness-shear motion with three nodes across the thickness of the plate rather than the one node of the fundamental thickness-shear mode. At about the same time, equations were developed which extended the classical (Lagrange–Germain–Cauchy) range of frequencies to include that of the fundamental thickness-shear mode; but it was not until much later Lee and Nikodem[2, 3] formulated equations suitable for studying vibrations at frequencies of the harmonic overtone modes of thickness-shear.

In the present paper, the Lee–Nikodem third-order equations are solved for a case of rotated-Y-cut quartz plates with free faces and a pair of parallel, free edges. The results of computations for the AT-cut plate are presented for vibrations in the neighborhood of the frequency of the fundamental thickness-shear mode and in the neighborhood of the third harmonic overtone. The differences between the two exhibit some of the reasons for the higher stability of the latter.

2. LEE-NIKODEM EQUATIONS

To obtain two-dimensional equations of motion of plates from the three-dimensional equations of linear elasticity, Lee and Nikodem start with an expansion of the three-dimensional, rectangular components of displacement, u_j , $j = 1, 2, 3$, in series of trigonometric functions of the thickness-coordinate, x_2 , of the plate:

$$u_j = \sum_{n=0}^{\infty} u_j^{(n)} \cos n\beta, \quad (1)$$

where the $u_j^{(n)}$ are independent of x_2 and

$$\beta = \pi(1 - x_2/b)/2, \quad (2)$$

in which b is the half-thickness of the plate. The functions $\cos n\beta$ give the shapes of the simple thickness-modes of an infinite, isotropic plate with free faces at $x_2 = \pm b$.

The expression (1), for the u_j , is substituted in the variational equation of motion[4]:

$$\int_V (T_{ij,i} - \rho \ddot{u}_j) \delta u_j \, dV = 0, \quad (3)$$

where the T_{ij} are the components of stress, ρ is the mass density and V is the volume. The integration is performed over the thickness of the plate and leads to stress-equations of motion of order n ; which are, omitting the terms accounting for surface tractions,

$$T_{ij}^{(n)} - (n\pi/2b) \bar{T}_{2j}^{(n)} = e_n \rho \ddot{u}_j^{(n)}, \quad (4)$$

where

$$T_{ij}^{(n)} = b^{-1} \int_{-b}^b T_{ij} \cos n\beta \, dx_2, \quad \bar{T}_{ij}^{(n)} = b^{-1} \int_{-b}^b T_{ij} \sin n\beta \, dx_2, \quad (5)$$

and $e_n = 2$ for $n = 0$ and $e_n = 1$ for $n > 0$. (Corrections of [3] by a factor of 2, for $n = 0$, were kindly supplied by Prof. Lee).

The three-dimensional strain-displacement relations,

$$S_{ij} = (u_{j,i} + u_{i,j})/2, \quad (6)$$

become, with (1),

$$S_{ij} = \sum_{n=0}^{\infty} (S_{ij}^{(n)} \cos n\beta + \bar{S}_{ij}^{(n)} \sin n\beta), \quad (7)$$

where

$$S_{ij}^{(n)} = (u_{j,i}^{(n)} + u_{i,j}^{(n)})/2, \quad \bar{S}_{ij}^{(n)} = n\pi(\delta_{2i}u_j^{(n)} + \delta_{2j}u_i^{(n)})/4b \quad (8)$$

and δ_{ij} is the Kronecker delta.

The three-dimensional stress-strain relations,

$$T_{ij} = c_{ijkl}S_{kl}, \quad i, j, k, l = 1, 2, 3 \quad \text{or} \quad T_p = c_{pq}S_q, \quad p, q = 1, \dots, 6, \quad (9)$$

become, from (5) and (6),

$$T_{ij}^{(n)} = c_{ijkl} \left(e_n S_{kl}^{(n)} + \sum_{m=1}^{\infty} A_{mn} \bar{S}_{kl}^{(m)} \right), \quad \bar{T}_{ij}^{(n)} = c_{ijkl} \left(\bar{S}_{kl}^{(n)} + \sum_{m=0}^{\infty} A_{nm} S_{kl}^{(m)} \right), \quad (10)$$

where

$$A_{mn} = 0, \quad m + n \text{ even}; \quad 4m/(m^2 - n^2)\pi, \quad m + n \text{ odd}. \quad (11)$$

The components of stress (10) are derivable from a strain energy density, U , according to

$$T_{ij}^{(n)} = \partial U / \partial S_{ij}^{(n)}, \quad \bar{T}_{ij}^{(n)} = \partial U / \partial \bar{S}_{ij}^{(n)}, \quad (12)$$

where

$$2U = c_{ijkl} \sum_{n=0}^{\infty} \left[e_n S_{ij}^{(n)} S_{kl}^{(n)} + \bar{S}_{ij}^{(n)} \bar{S}_{kl}^{(n)} + \sum_{m=0}^{\infty} (A_{mn} S_{ij}^{(n)} \bar{S}_{kl}^{(m)} + A_{nm} \bar{S}_{ij}^{(n)} S_{kl}^{(m)}) \right]. \quad (13)$$

3. REDUCTION TO A SPECIAL CASE

The example to be studied is one of steady vibrations at frequencies high enough to include the third harmonic overtone of the thickness-shear family of modes of an AT-cut quartz plate bounded by free faces at $x_2 = \pm b$ and free edges at $x_1 = \pm a$. The modes are to be straight-crested along x_3 and antisymmetric with respect to both x_1 and x_2 . Thus, we take, of (1), only

$$\begin{aligned} u_1 &= (u_1^{(1)} \cos \beta + u_1^{(3)} \cos 3\beta) e^{i\omega t}, \\ u_2 &= (u_2^{(0)} + u_2^{(2)} \cos 2\beta) e^{i\omega t}, \\ u_3 &= (u_3^{(0)} + u_3^{(2)} \cos 2\beta) e^{i\omega t}, \end{aligned} \quad (14)$$

in which the $u_j^{(n)}$ depend only on x_1 . The second term in u_1 accommodates the third harmonic overtone thickness-shear mode.

What remain of the stress-equations of motion (4) are

$$\begin{aligned}
 T_{12,1}^{(0)} + 2\rho\omega^2 u_2^{(0)} &= 0, & T_{13,1}^{(0)} + 2\rho\omega^2 u_3^{(0)} &= 0, \\
 T_{11,1}^{(1)} - (\pi/2b)\bar{T}_{21}^{(1)} + \rho\omega^2 u_1^{(1)} &= 0, & T_{12,1}^{(2)} - (\pi/b)\bar{T}_{22}^{(2)} + \rho\omega^2 u_2^{(2)} &= 0, \\
 T_{13}^{(2)} - (\pi/b)\bar{T}_{23}^{(2)} + \rho\omega^2 u_3^{(2)} &= 0, & T_{11,1}^{(3)} - (3\pi/2b)\bar{T}_{21}^{(3)} + \rho\omega^2 u_1^{(3)} &= 0
 \end{aligned} \tag{15}$$

and the only non-zero components of strain are, from (8) and (14),

$$\begin{aligned}
 S_5^{(0)} &= u_{3,1}^{(0)}, & S_6^{(0)} &= u_{2,1}^{(0)}, \\
 S_1^{(1)} &= u_{1,1}^{(1)}, & \bar{S}_6^{(1)} &= (\pi/2b)u_1^{(1)}, \\
 S_5^{(2)} &= u_{3,1}^{(2)}, & S_6^{(2)} &= u_{2,1}^{(2)}, \\
 \bar{S}_2^{(2)} &= (\pi/b)u_2^{(2)}, & \bar{S}_4^{(2)} &= (\pi/b)u_3^{(2)}, \\
 S_1^{(3)} &= u_{1,1}^{(3)}, & \bar{S}_6^{(3)} &= (3\pi/2b)u_1^{(3)}.
 \end{aligned} \tag{16}$$

Nine constants of elasticity, referred to axes in and normal to the plane of the plate (with x_1 an axis of two-fold symmetry of the elastic properties of quartz) enter into the present example. As computed by Ballato[5] from Bechmann's[6] principal constants, they are (in $\text{N/m}^2 \times 10^{-9}$):

$$\begin{array}{lll}
 c_{11} = 86.74 & c_{12} = -8.260543013 & c_{55} = 68.80698505 \\
 c_{22} = 129.7663387 & c_{24} = 5.700423178 & c_{66} = 29.01301496 \\
 c_{44} = 38.61152627 & c_{14} = -3.654869573 & c_{56} = 2.533571817.
 \end{array}$$

Of the remaining twelve constants, four (c_{13} , c_{23} , c_{33} , c_{43}) do not enter into the present example, as the modes are independent of x_3 ; and the others (c_{15} , c_{25} , c_{35} , c_{45} , c_{16} , c_{26} , c_{36} , c_{46}) are zero for the rotated-Y-cuts of quartz.

Lee and Nikodem introduce a low frequency correction factor k_1 and a high frequency correction factor k_2 . The former appears as a factor of A_{10} in the strain energy density appropriate to the present example:

$$\begin{aligned}
 2U &= 2(c_{55}S_5^{(0)}S_5^{(0)} + c_{66}S_6^{(0)}S_6^{(0)} + 2c_{56}S_5^{(0)}S_6^{(0)} + c_{11}S_1^{(1)}S_1^{(1)} \\
 &+ c_{55}S_5^{(2)}S_5^{(2)} + c_{66}S_6^{(2)}S_6^{(2)} + 2c_{56}S_5^{(2)}S_6^{(2)} + c_{11}S_1^{(3)}S_1^{(3)} \\
 &+ c_{22}\bar{S}_2^{(2)}\bar{S}_2^{(2)} + c_{44}\bar{S}_4^{(2)}\bar{S}_4^{(2)} + 2c_{24}\bar{S}_2^{(2)}\bar{S}_4^{(2)} + c_{66}\bar{S}_6^{(1)}\bar{S}_6^{(1)} + c_{66}\bar{S}_6^{(3)}\bar{S}_6^{(3)} \\
 &+ 2k_1A_{10}(c_{66}S_6^{(0)} + c_{56}S_5^{(0)})\bar{S}_6^{(1)} + 2A_{12}(c_{66}S_6^{(2)} + c_{56}S_5^{(2)})\bar{S}_6^{(1)} \\
 &+ 2A_{21}(c_{12}\bar{S}_2^{(2)} + c_{14}\bar{S}_4^{(2)})S_1^{(1)} + 2A_{23}(c_{12}\bar{S}_2^{(2)} + c_{14}\bar{S}_4^{(2)})S_1^{(3)} \\
 &+ 2A_{30}(c_{66}S_6^{(0)} + c_{56}S_5^{(0)})\bar{S}_6^{(3)} + 2A_{32}(c_{66}S_6^{(2)} + c_{56}S_5^{(2)})\bar{S}_6^{(3)},
 \end{aligned} \tag{17}$$

where

$$\begin{aligned}
 A_{10} &= 4/\pi, & A_{12} &= -4/3\pi & A_{21} &= 8/3\pi, \\
 A_{23} &= -8/5\pi, & A_{30} &= 4/3\pi, & A_{32} &= 12/5\pi.
 \end{aligned} \tag{18}$$

The correction factor k_2 , in the present example, is inserted as a divisor of the term $2\rho\omega^2 u_2^{(0)}$ in the first of (15).

Adjusted values of k_1 and k_2 , as supplied by Professor Lee, are

$$k_1^2 = \pi^2/8, \quad k_2^{1/2} = 0.901. \tag{19}$$

From (12), (17) and (16), the surviving stress-displacement relations are

$$\begin{aligned}
 T_{13}^{(0)} &= 2[c_{55}u_{3,1}^{(0)} + c_{56}(u_{2,1}^{(0)} + k_1 b^{-1} u_1^{(1)} + b^{-1} u_1^{(3)})], \\
 T_{12}^{(0)} &= 2[c_{56}u_{3,1}^{(0)} + c_{66}(u_{2,1}^{(0)} + k_1 b^{-1} u_1^{(1)} + b^{-1} u_1^{(3)})], \\
 T_{11}^{(1)} &= c_{11}u_{1,1}^{(1)} + (8/3b)(c_{12}u_2^{(2)} + c_{14}u_3^{(2)}), \\
 T_{13}^{(2)} &= c_{55}u_{3,1}^{(2)} + c_{56}[u_{2,1}^{(2)} - (2/3b)u_1^{(1)} + (18/5b)u_1^{(3)}], \\
 T_{12}^{(2)} &= c_{56}u_{3,1}^{(2)} + c_{66}[u_{2,1}^{(2)} - (2/3b)u_1^{(1)} + (18/5b)u_1^{(3)}], \\
 T_{11}^{(3)} &= c_{11}u_{1,1}^{(3)} - (8/5b)(c_{12}u_2^{(2)} + c_{14}u_3^{(2)}), \\
 \bar{T}_{12}^{(1)} &= (4k_1/\pi)(c_{56}u_{3,1}^{(0)} + c_{66}u_{2,1}^{(0)}) + (\pi/2b)c_{66}u_1^{(1)} - (4/3\pi)(c_{56}u_{3,1}^{(2)} + c_{66}u_{2,1}^{(2)}), \\
 \bar{T}_{22}^{(2)} &= (8/\pi)c_{12}(u_{1,1}^{(1)}/3 - u_{1,1}^{(3)}/5) + (\pi/b)(c_{22}u_2^{(2)} + c_{24}u_3^{(2)}), \\
 T_{23}^{(1)} &= (8/\pi)c_{14}(u_{1,1}^{(1)}/3 - u_{1,1}^{(3)}/5) + (\pi/b)(c_{24}u_2^{(2)} + c_{44}u_3^{(2)}), \\
 \bar{T}_{12}^{(3)} &= (4/3\pi)(c_{56}u_{3,1}^{(0)} + c_{66}u_{2,1}^{(0)}) + (12/5\pi)(c_{56}u_{3,1}^{(2)} + c_{66}u_{2,1}^{(2)}) + (3\pi/2b)c_{66}u_1^{(3)}.
 \end{aligned} \tag{20}$$

The displacement equations of motion, to be solved, are obtained by substituting the stress-displacement relations (20) into the stress-equations of motion (15)—with k_2 inserted in the first of (15), as mentioned previously.

Finally, the edge conditions are

$$T_{13}^{(0)} = T_{12}^{(0)} = T_{11}^{(1)} = T_{13}^{(2)} = T_{12}^{(2)} = T_{11}^{(3)} = 0 \quad \text{on} \quad x_1 = \pm a. \tag{21}$$

4. DISPERSION RELATION

In (14) we take, omitting the factor $e^{i\omega t}$,

$$\begin{aligned}
 u_2^{(0)} &= A_2^{(0)} \sin \xi x_1, & u_2^{(2)} &= A_2^{(2)} \sin \xi x_1, \\
 u_3^{(0)} &= A_3^{(0)} \sin \xi x_1, & u_3^{(2)} &= A_3^{(2)} \sin \xi x_1, \\
 u_1^{(1)} &= A_1^{(1)} \cos \xi x_1, & u_1^{(3)} &= A_1^{(3)} \cos \xi x_1
 \end{aligned} \tag{22}$$

and substitute first in (20) and the result in (15) to produce a set of six simultaneous, homogeneous, linear algebraic equations in the six amplitudes $A_j^{(n)}$ of (22):

$$\begin{aligned}
 a_{11}A_2^{(0)} + a_{12}A_3^{(0)} + a_{13}A_1^{(1)} + 0 + 0 + a_{16}A_1^{(3)} &= 0 \\
 a_{12}A_2^{(0)} + a_{22}A_3^{(0)} + a_{23}A_1^{(1)} + 0 + 0 + a_{26}A_1^{(3)} &= 0 \\
 a_{13}A_2^{(0)} + a_{23}A_3^{(0)} + a_{33}A_1^{(1)} + a_{34}A_2^{(2)} + a_{35}A_3^{(2)} + 0 &= 0 \\
 0 + 0 + a_{34}A_1^{(1)} + a_{44}A_2^{(2)} + a_{45}A_3^{(2)} + a_{46}A_1^{(3)} &= 0 \\
 0 + 0 + a_{35}A_1^{(1)} + a_{45}A_2^{(2)} + a_{55}A_3^{(2)} + a_{56}A_1^{(3)} &= 0 \\
 a_{16}A_2^{(0)} + a_{26}A_3^{(0)} + 0 + a_{46}A_2^{(2)} + a_{56}A_3^{(2)} + a_{66}A_1^{(3)} &= 0.
 \end{aligned} \tag{23}$$

The coefficients a_{pq} , made dimensionless and real by some manipulations of the equations, are

$$\begin{aligned}
 a_{11} &= 2(z^2 - \Omega^2/k_2), & a_{12} &= 2\bar{c}_{56}z^2, & a_{13} &= 4k_1z^2/\pi, & a_{16} &= 4z^2/\pi, \\
 a_{22} &= 2(\bar{c}_{55}z^2 - \Omega^2), & a_{23} &= 4k_1\bar{c}_{56}z^2/\pi, & a_{26} &= 4\bar{c}_{56}z^2/\pi, \\
 a_{33} &= (\bar{c}_{11}z^2 + 1 - \Omega^2)z^2, & a_{34} &= -4(1 + 4\bar{c}_{12})z^2/3\pi, & a_{35} &= 4(4\bar{c}_{14} - \bar{c}_{56})z^2/3\pi, \\
 a_{44} &= z^2 + 4\bar{c}_{22} - \Omega^2, & a_{45} &= 4\bar{c}_{24} + \bar{c}_{56}z^2, & a_{46} &= 4(9 + 4\bar{c}_{12})z^2/5\pi, \\
 a_{55} &= \bar{c}_{55}z^2 + 4\bar{c}_{44} - \Omega^2, & a_{56} &= 4(4\bar{c}_{14} + 9\bar{c}_{56})z^2/5\pi, \\
 a_{66} &= (\bar{c}_{11}z^2 + 9 - \Omega^2)z^2,
 \end{aligned} \tag{24}$$

where

$$z = 2\xi b/\pi, \quad \Omega = \omega/\bar{\omega}, \quad \bar{\omega}^2 = \pi^2 c_{66}/4\rho b^2, \quad \bar{c}_{pq} = c_{pq}/c_{66};$$

i.e. z is the ratio of the thickness of the plate to the half-wave-length along the plate and Ω is the ratio of the frequency to that of the fundamental thickness-shear mode of the infinite plate.

The determinant of the coefficients of the $A_j^{(n)}$, set equal to zero:

$$|a_{pq}| = 0, \quad (25)$$

in which $a_{14} = a_{15} = a_{24} = a_{25} = a_{36} = 0$, $a_{pq} = a_{qp}$, produces the dispersion relation Ω vs z : a sextic, algebraic equation in z^2 . The equation is the same as (43) of [3] except for the factors 2 in a_{11} , a_{12} , a_{22} as already noted above in connection with (4). Also, here, all the elements a_{pq} are real as a result of multiplication of the third and sixth rows and columns by z .

The six branches of the dispersion relation, computed on the HP-85 micro-computer, are illustrated in Fig. 1. The characters of the branches are indicated by their identifying symbols:

- F = Flexure
- FS = Face-shear
- 1_1 = 1st Thickness-shear (in x_1 -direction)
- 2_3 = 2nd Thickness-shear (in x_3 -direction)
- 3_1 = 3rd (Harmonic) Thickness-shear (in x_1 -direction)
- 2_2 = 2nd Thickness-stretch (in x_2 -direction).

The subscripts in the symbols 1_1 , 2_3 , 3_1 , 2_2 , designate the direction of displacement (or predominant displacement) at $z = 0$, whereas the numbers themselves give the number of nodes between $x_2 = \pm b$. Thus: in 2_3 the displacement at $z = 0$ is predominantly in the direction of x_3 with two nodes across the thickness of the plate. Note that the roots z for branches F and FS are real for all Ω , but the roots for the remaining four branches may be real or imaginary, depending on the frequency. If imaginary, the variation of displacement along x_1 is exponential or hyperbolic rather than trigonometric.

The zigzags in the curves in Fig. 1 result from the spacing of dots on the cathode ray tube display of the HP-85. The figure is the HP-85's hard copy of the CRT display. The roots z were actually computed to an accuracy of 10^{-9} —a precision required for their subsequent use in solving (34) and (37). Intervals of 0.02 in Ω were employed for Fig. 1, resulting in a computation time, for the range $0 < \Omega < 4$, of about 6 hr or about 18 sec per root. The secant iterative method

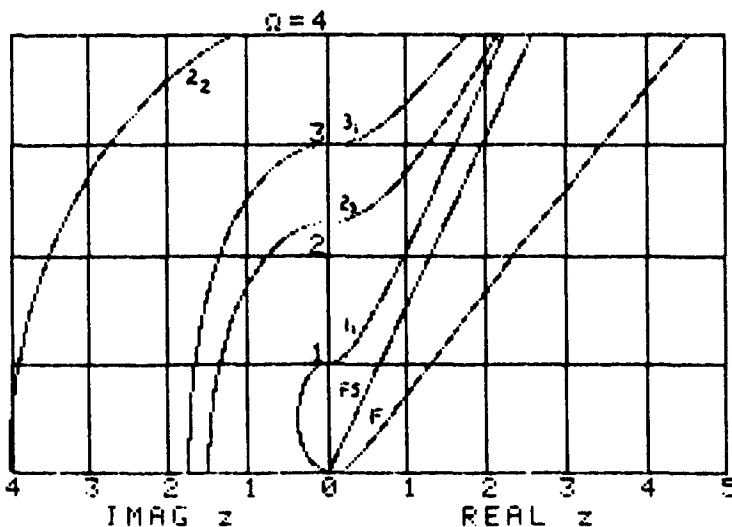


Fig. 1. Dispersion curves for waves in an infinite AT-cut quartz plate.

was used, with starting values given by the following approximate formulas, followed by increments of 10^{-6} in z_n^2 :

$$\left. \begin{matrix} F: z_1^2 \\ 1_1: z_3^2 \end{matrix} \right\} = 6.42258(1 + G)\Omega^2[1 \pm (1 + K)^{1/2}]/\pi^2, \tag{26}$$

$$G = \pi^2/12(\bar{c}_{11} - \bar{c}_{12}^2/\bar{c}_{22}), \quad K = 4G(\Omega^{-2} - 1)/(1 + G)^2, \tag{27}$$

$$FS: z_2^2 = 0.44119\Omega^2, \tag{28}$$

$$2_3: z_4^2 = \begin{cases} 2.229(\Omega^2/\Omega_4^2 - 1), & \Omega < \Omega_4, \\ 0.42395(\Omega^2/\Omega_4^2 - 1), & \Omega > \Omega_4, \end{cases} \tag{29}$$

$$2_2: z_6^2 = 16(\Omega^2/\Omega_6^2 - 1), \quad \Omega < \Omega_6, \tag{30}$$

$$\Omega_4^2, \Omega_6^2 = 2\{\bar{c}_{22} + \bar{c}_{44} \mp [(\bar{c}_{22} - \bar{c}_{44})^2 + 4\bar{c}_{24}^2]^{1/2}\}, \tag{31}$$

$$3_1: z_5^2 = \begin{cases} 0.33799(\Omega^2 - 9), & \Omega < 3, \\ 0.40651(\Omega^2 - 9), & \Omega > 3. \end{cases} \tag{32}$$

These trial roots match closely or exactly the roots of the sextic at $z = 0$ and at $\Omega = 0, 3$ (except z_6 at $\Omega = 3$) resulting in trial values adequate for convergence of the iteration for all $0 < \Omega < 4$.

5. FREQUENCY SPECTRUM

For each of the roots z_n^2 of (25), five amplitude ratios, say

$$A_2^{(0)}/A_1^{(1)} = \alpha_{1n}, \quad A_3^{(0)}/A_1^{(1)} = \alpha_{2n}, \quad A_2^{(2)}/A_1^{(1)} = \alpha_{3n}, \quad A_3^{(2)}/A_1^{(1)} = \alpha_{4n}, \quad A_1^{(3)}/A_1^{(1)} = \alpha_{5n}, \tag{33}$$

may be found from five of the six equations (23). Thus, with the third of (23) omitted, we may write

$$\begin{aligned} a_{11}(z_n\alpha_{1n}) + a_{12}(z_n\alpha_{2n}) + 0 + 0 + a_{16}\alpha_{5n} &= -a_{13} \\ a_{12}(z_n\alpha_{1n}) + a_{22}(z_n\alpha_{2n}) + 0 + 0 + a_{26}\alpha_{5n} &= -a_{23} \\ 0 + 0 + a_{44}(z_n\alpha_{3n}) + a_{45}(z_n\alpha_{4n}) + a_{46}\alpha_{5n} &= -a_{34}, \\ 0 + 0 + a_{45}(z_n\alpha_{3n}) + a_{55}(z_n\alpha_{4n}) + a_{56}\alpha_{5n} &= -a_{35} \\ a_{16}(z_n\alpha_{1n}) + a_{26}(z_n\alpha_{2n}) + a_{46}(z_n\alpha_{3n}) + a_{56}(z_n\alpha_{4n}) + a_{66}\alpha_{5n} &= 0. \end{aligned} \tag{34}$$

This form is chosen because the $z_n\alpha_{1n}, z_n\alpha_{2n}, z_n\alpha_{3n}, z_n\alpha_{4n}$ and α_{5n} are real for all Ω , as are also the a_{pq} —as arranged previously.

With the six z_n from (25) and the thirty α_{pn} determined from (34), we may now write, in place of (22):

$$\begin{aligned} u_2^{(0)} &= \sum_{n=1}^6 A_n\alpha_{1n} \sin \xi_n x_1, & u_3^{(0)} &= \sum_{n=1}^6 A_n\alpha_{2n} \sin \xi_n x_1, \\ u_1^{(1)} &= \sum_{n=1}^6 A_n \cos \xi_n x_1, & u_2^{(2)} &= \sum_{n=1}^6 A_n\alpha_{3n} \sin \xi_n x_1, \\ u_3^{(2)} &= \sum_{n=1}^6 A_n\alpha_{4n} \sin \xi_n x_1, & u_1^{(3)} &= \sum_{n=1}^6 A_n\alpha_{5n} \cos \xi_n x_1. \end{aligned} \tag{35}$$

Upon substituting the displacements (35) in the formulas (20) for the stresses and the results in the edge conditions (21), we have the six equations:

$$\sum_{n=1}^6 A_n b_{mn} = 0, \quad m = 1, \dots, 6, \tag{36}$$

where

$$\begin{aligned}
 b_{1n} &= (\bar{c}_{56}z_n\alpha_{1n} + \bar{c}_{55}z_n\alpha_{2n} + 2k_1\bar{c}_{56}/\pi + 2\bar{c}_{56}\alpha_{5n}/\pi) \cos \hat{z}_n l, \\
 b_{2n} &= (z_n\alpha_{1n} + \bar{c}_{56}z_n\alpha_{2n} + 2k_1/\pi + 2\alpha_{5n}/\pi) \cos \hat{z}_n l, \\
 b_{3n} &= (-\bar{c}_{11}z_n^2 + 16z_n\alpha_{3n}/3 + 16\bar{c}_{14}z_n\alpha_{4n}/3)\hat{z}_n^{-1} \sin \hat{z}_n l, \\
 b_{4n} &= (-4\bar{c}_{56}/3\pi + \bar{c}_{56}z_n\alpha_{3n} + \bar{c}_{55}z_n\alpha_{4n} + 36\bar{c}_{56}\alpha_{5n}/5\pi) \cos \hat{z}_n l, \\
 b_{5n} &= (-4/3\pi + z_n\alpha_{3n} + \bar{c}_{56}z_n\alpha_{4n} + 36\alpha_{5n}/5\pi) \cos \hat{z}_n l, \\
 b_{6n} &= (16\bar{c}_{12}z_n\alpha_{3n}/5\pi + 16\bar{c}_{14}z_n\alpha_{4n}/5\pi + \bar{c}_{11}z_n^2\alpha_{5n})\hat{z}_n^{-1} \sin \hat{z}_n l,
 \end{aligned}$$

in which $\hat{z}_n = \pi z_n/2 = \xi_n b$, $l = a/b$ and the b_{mn} are real for all Ω .

The roots l of the equation obtained by setting the 6×6 determinant of the coefficients of the A_n , in (36), equal to zero:

$$|b_{mn}| = 0, \tag{37}$$

produce the data for plotting a frequency spectrum Ω vs a/b .

The results of computations in the two ranges

$$0.99 < \Omega < 1.01, \quad 16 < a/b < 24$$

and

$$2.995 < \Omega < 3.005, \quad 18 < a/b < 22$$

are illustrated in Figs. 2 and 3. To construct these figures, the six roots z_n of the sextic (25) were first computed for a given Ω . Then the five linear equations (34) were solved for the α_{pn} for each of the six z_n and the resulting combinations of α_{pn} and z_n substituted in the transcendental equation (37), after which the range of $l (= a/b)$ was traversed in steps of 0.1 for Fig. 2 and 0.025 for Fig. 3 and the values of $|b_{mn}|$ computed at each step. A change of sign of $|b_{mn}|$ indicated a straddled root l which was then determined to 10^{-3} by successive linear interpolations. The process was then repeated at intervals of Ω of 5×10^{-5} . Figures 2 and 3 required about 58 and 49 hr of computation, respectively, on the HP-85.

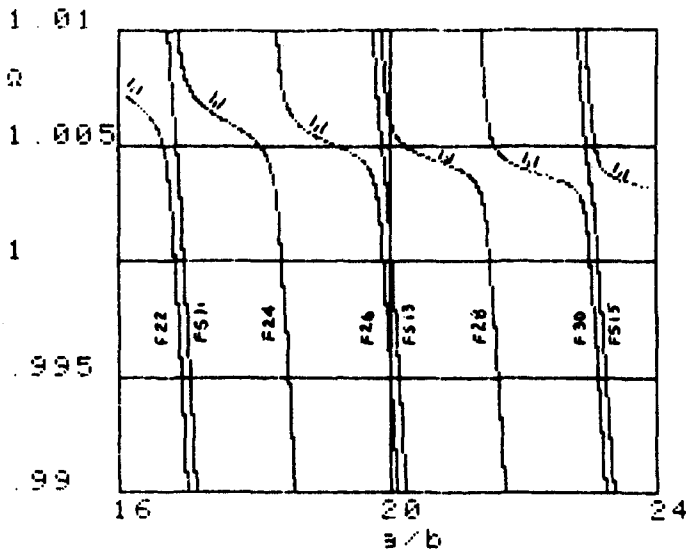


Fig. 2. Frequency spectrum—AT-cut quartz strip with free edges—in the neighborhood of the fundamental thickness-shear mode.

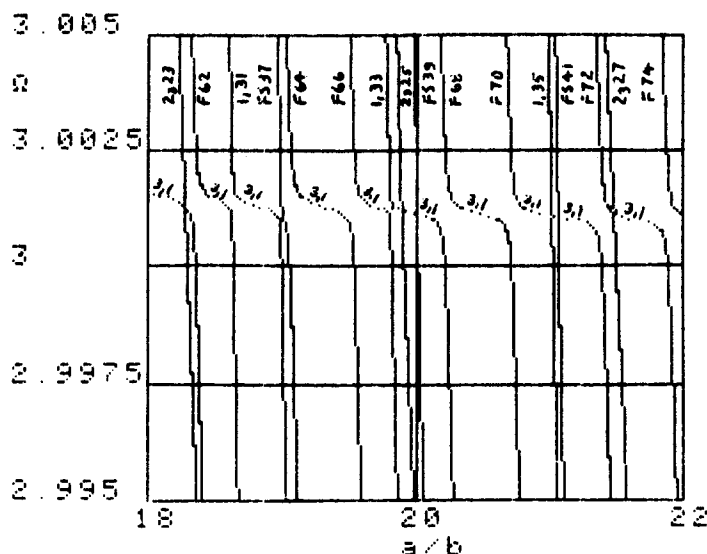


Fig. 3. Frequency spectrum—AT-cut quartz strip with free edges—in the neighborhood of the third harmonic thickness-shear overtone mode.

In Fig. 2:

- $F\ 22, \dots, 30$ are overtones of flexure
- $FS\ 11, \dots, 15$ are overtones of face-shear
- $1_1, 1$ is the 1st thickness-shear (fundamental).

In Fig. 3:

- $F\ 62, \dots, 74$ are overtones of flexure
- $FS\ 37, \dots, 41$ are overtones of face-shear
- $1_1, 3, 3, \dots, 35$ are anharmonic overtones of the 1st (fundamental) thickness-shear
- $2_1, 3, 3, \dots, 27$ are anharmonic overtones of the 2nd transverse thickness-shear
- $3_1, 1$ is the 3rd harmonic thickness-shear overtone.

The numbers following the symbols F , FS , 1_1 , 2_1 , and 3_1 designate both the order of the overtone and the approximate number of half-wave-lengths between $x_1 = \pm a$.

Figure 2 illustrates the well known phenomenon of strong coupling of the 1st thickness-shear fundamental with flexure overtones and weak coupling with face-shear overtones. Figure 3 shows that the 3rd harmonic thickness-shear mode has moderately strong coupling with flexure overtones and weak coupling with face-shear overtones and, in addition, weak coupling with transverse thickness-shear overtones. As for the interaction of the 3rd harmonic thickness-shear overtone with the anharmonic overtones of the fundamental thickness shear, the coupling is moderately strong at small a/b (thick plates and low order anharmonic overtones) and diminishes as a/b increases (thin plates and increasing order of anharmonic overtones).

Finally, the minimum absolute values of the slopes of the segments $1_1, 1$ are much larger than those of $3_1, 1$. For large a/b , the ratio of those slopes is approximated by the ratio of the curvatures of branches 3_1 and 1_1 at $z = 0$ in Fig. 1. The exact values of those curvatures, in the three-dimensional theory, were given by Ekstein[7, eqn (56)]:

$$\kappa_n = [d^2\Omega/dz^2]_{z=0} = k + C \cot(n\pi/2c_2^{1/2}) + D \cot(n\pi/2c_3^{1/2}),$$

where

$$\begin{aligned}
 k &= (\bar{c}_{11} + A + B), \quad n = 1, 3, 5, \dots, \\
 A &= [(1 + \bar{c}_{12}) \cos \theta + (\bar{c}_{14} + \bar{c}_{56}) \sin \theta]^2 / (1 - c_2), \\
 B &= [(\bar{c}_{14} + \bar{c}_{56}) \cos \theta - (1 + \bar{c}_{12}) \sin \theta]^2 / (1 - c_3), \\
 C &= 4[(c_2 + \bar{c}_{12}) \cos \theta + (c_2 \bar{c}_{56} + \bar{c}_{14})]^2 / n^2 \pi c_2^{1/2} (1 - c_2)^2, \\
 D &= 4[(c_3 + \bar{c}_{12}) \sin \theta - (c_3 \bar{c}_{56} + \bar{c}_{14})]^2 / n^2 \pi c_2^{1/2} (1 - c_3)^2, \\
 c_2, c_3 &= \{\bar{c}_{22} + \bar{c}_{44} \pm [(\bar{c}_{22} - \bar{c}_{44})^2 + 4\bar{c}_{24}^2]^{1/2}\} / 2, \\
 \tan \theta &= \bar{c}_{24} / (c_2 - \bar{c}_{44}).
 \end{aligned}$$

For the present case, the curvature ratio κ_1/κ_3 is 4.7 and that is the ratio of the slopes.

The large ratio of slopes and the absence, at large a/b , of strong coupling with all overtones except those of flexure (which, at such high overtones, have very small amplitudes) are important contributors to the high stability of third harmonic overtone resonators.

Acknowledgement—This work was sponsored by the Department of the Navy, Office of Naval Research, Structural Mechanics Program, Contract N00014-80-C-0559.

REFERENCES

1. A. W. Warner, High frequency crystal units for primary frequency standards. *Proc. I.R.E.* **40**, 1030 (1952).
2. P. C. Y. Lee and Z. Nikodem, An approximate theory for high-frequency vibrations of elastic plates. *Int. J. Solids Structures* **8**, 581 (1972).
3. Z. Nikodem and P. C. Y. Lee, Approximate theory of vibrations of crystal plates at high frequencies. *Int. J. Solids Structures* **10**, 177 (1974).
4. A. E. H. Love, *A Treatise on the Mathematical Theory of Elasticity*, 4th Edn, p. 166. Cambridge, University Press, London (1927).
5. A. Ballato, private communication.
6. R. Bechmann, Elastic and piezoelectric constants of alpha-quartz. *Phys. Rev.* **110**, 1060 (1950).
7. H. Ekstein, High frequency vibrations of thin crystal plates. *Phys. Rev.* **68**, 11 (1945).